

# **METODE DE PROIECTARE PENTRU SISTEME DE REGLARE AUTOMATA**

Prof. Dr. Ing. Dipl. Math. Dr. h.c. mult. Radu-Emil Precup

<https://www.aut.upt.ro/~rprecup/>

# Outline

## Controller designs for time delay systems and for slow processes

- Tuning Method Based on Reaching the Stability Margin
- Tuning Method Based on the Relations Due to Oppelt or Chien-Hrones-Reswick
- Strejc's Method
- Using the Smith Predictor
- Application

## Modulus Optimum method and Symmetrical Optimum method

- A short overview of the Symmetrical Optimum method
- A practical version of the Symmetrical Optimum method
- Extensions of the Symmetrical Optimum method
  - The Extended Symmetrical Optimum method (the ESO method)
  - The double parameterization of the SO method (the 2p-SO method)
- Sensitivity analysis in the frequency domain
- Further performance enhancement. Alternative controller structures.
- Equivalency of 1 DOF (PID) and 2 DOF controllers
- Application

# 1

## **Controller designs for time delay systems and for slow processes**



For numerous industrial control applications, it is possible to determine the dynamics of the process by applying a step (deterministic input) and study its response

The simplest parametric models (benchmark-type models, assuming a monotonically changing output process, are the three or four parameter models)

Example of transfer function (t.f.) of benchmark-type model:

$$P(s) = \frac{k_P}{1+sT} e^{-sT_m} \quad (4.1.1)$$

where:

- $k_P$  – the process static gain
- $T$  – the time constant and  $T_m$  – the dead time (or the transport lag or the time delay)

The model (4.1.1) = first order lag plus dead time (FOLDT) or first order plus time delay (FOPTD)

Many design approaches for one-degree-of-freedom (1-DOF) controllers have been developed for these types of benchmark-type models. The majority of industrial applications with 1-DOF controllers is actually using PI and PID controllers

The design approaches of 1-DOF controllers for processes that can be characterized by t.f.s in the forms such as (4.1.1) can be organized as follows (didactical wise):

- Methods based on previously calculated empirical relations (e.g., Ziegler-Nichols) based on the control system (CS) structure given in Fig. 4.1.1 (a)
- Frequency domain methods based on the CS structure given in Fig. 4.1.1 (a)
- Methods applied to the case of internal model control (IMC) structures in their version with Smith predictor in the framework of the CS structure given in Fig. 4.1.1 (b)

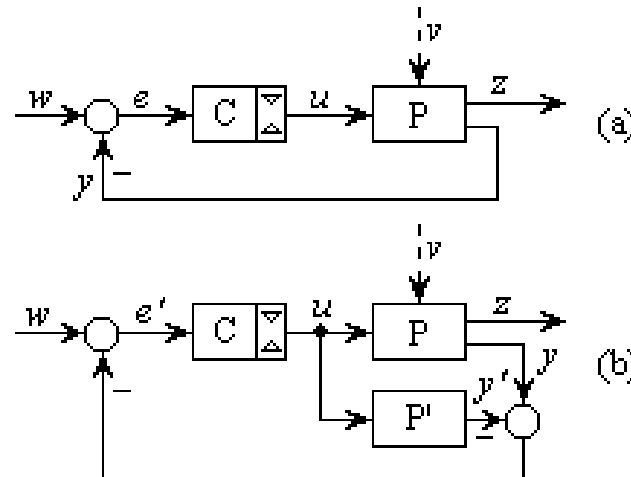


Fig. 4.1.1:

# Tuning method based on reaching the stability margin

This method is advantageous due to the fact that it does not require the knowing of the mathematical model (MM) of the process. In turn, it is subjected to constraints concerning the piecewise linearity and the saturation entering of the controller

The procedure that has to be followed is:

- 1) The control loop is closed using a proportional controller (with the gain  $k_R^P$ ) and the plant (the process) is determined to get in steady-state operating regime
- 2) The value of  $k_R^P$  is increased step by step until the control loop enters a regime characterized by permanent oscillations with the period  $T_0$
- 3) The recommended controller types are chosen accounting for the nature of the plant and the particular features concerning its control
- 4) The use of the specific relations given by Ziegler and Nichols: the values  $\{k_{R0}^P, T_0\}$  are employed in the computation of the values of the tuning parameters  $\{k_R, T_i, T_d\}$  or  $\{k_p, k_i, k_d\}$  of the PI or PID controller:

$$C(s) = k_R \left( 1 + \frac{1}{sT_i} + \frac{sT_d}{1+sT_f} \right), T_f \ll T_d \quad (4.1.4)$$

$$C(s) = k_p + \frac{k_i}{s} + k_d \frac{s}{1+sT_f}$$

with  $k_d = T_d = 0$  for the PI controller

- 5) The designer will construct the implementation diagram of the controller and he/she will conduct experiments related to the study of the system behavior

## Tuning method based on reaching the stability margin (cont.)

6) The empirical performance indices, i.e., overshoot ( $\sigma_1$ ), settling time ( $t_s$ ) and natural static coefficient ( $\gamma$ ), are used in the assessment of the system quality

7) The behavior of the designed CS (with the tuned parameters) is compared with the behavior of a system with modified controller tuning parameters (sensitivity analysis):

$$k_R = k_{R0} \pm \Delta k_R, T_i = T_{i0} + \Delta T_i, T_d = T_{d0} \pm \Delta T_d \quad (4.1.5)$$

8) It is recommended next to design an Anti-Reset-Windup (ARW) measure and to study the effects of its implementation



## Tuning method based on the relations due to Oppelt or Chien-Hrones-Reswick

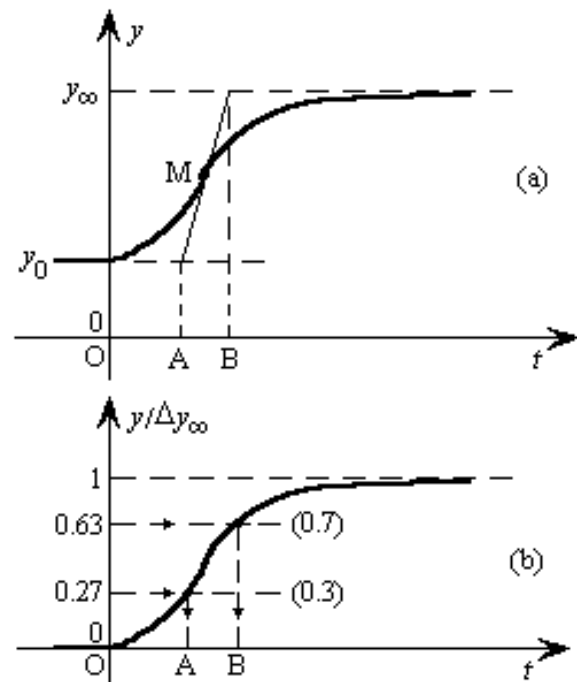
If the process is subjected to open loop identification by the step response method under the form of the model  $P(s)$  given in (4.1.1), one of the following methods is recommended to compute the process parameters:

- the tangent method – Fig. 4.1.3 (a), where:

$$k_P = \Delta y_\infty / \Delta u_\infty, T = \overline{OA}, T_m = \overline{AB} \quad (4.1.11)$$

- data-driven system identification

Fig. 4.1.3:





## Strejc's method

This method has the specific feature that in some certain conditions the MM of the process (the plant) is in the form (4.1.2) or (4.1.3), where the dead time  $T_m$  is a real one or a computational one. The controller design methods are various and often dedicated to some classes of applications:

$$P(s) = \frac{k_P}{(1 + sT)^2} e^{-sT_m} \quad (4.1.2)$$

$$P(s) = \frac{k_P}{(1+sT_1)(1+sT_2)} e^{-sT_m} \quad (4.1.3)$$

## Using the Smith predictor

The study and implementation of the control structures based on Smith predictor (Fig. 4.1.1 (b)) have an advantage in the simultaneous treatment of the idea of IMC and the prediction based on the anticipation effect. The MM of the plant is separated in its two components (rational part and the component that characterizes the dead time):

(4.1.14)

$$P(s) = P'(s)e^{-sT_m}$$

The result is the separation of the design of the controller  $C(s)$  relative to the part  $P'(s)$

Two controller tuning methods can be applied:

- 1) The analytical design in the frequency domain
- 2) The design based on the application of the Modulus Optimum method or of the Extended Symmetrical Optimum (adapted to the plants without integral component)

The following steps are used in this first method:

- 1) The experimental identification by the step response method (in different operating conditions)
- 2) The acceptance of the control solution based on the PI controller with the t.f.

$$C(s) = \frac{k_c}{s} (1 + sT_c) \quad (4.1.15)$$

## Using the Smith predictor (cont.)

3) The determination of the frequency response function and of its magnitude and phase functions:

$$|H_0(j\omega)| = (k_c k_p / \omega) \sqrt{\frac{1 + (\omega T_c)^2}{1 + (\omega T)^2}} \quad (4.1.16)$$

$$\arg H_0(j\omega) = \frac{\pi}{2} + \tan^{-1}(\omega T_c) - \tan^{-1}(\omega T)$$

4) The imposing of a desired phase margin, and the calculation of the crossover frequency  $\omega_c$

5) The calculation of the tuning parameters  $\{k_c, T_c\}$  (or  $\{k_R, T_R\}$ ) – not a single solution

6) The calculation of the feedback compensator, with the t.f.  $C_c(s)$ , using the first order Pade approximation



## Application 4.1.1

The equipment “Air Stream and Temperature Control Plant” (ASTCP, Fig. 4.1.4) – a multifunctional product, which can ensure the control of two parameters, the air temperature and air stream

The functional block diagram of the ASTCP – Fig. 4.1.5. The strictly speaking plant is characterized by:

- two input variables: the ventilator (or the fan) motor speed and the control signal of the heating element
- five measurable variables: the air stream, the air temperature (in two points), the air pressure and the position of the air admission throttle

In this context, the equipment permits the construction of numerous control structures for temperature and air stream control

Fig. 4.1.4:





## Application (cont.)

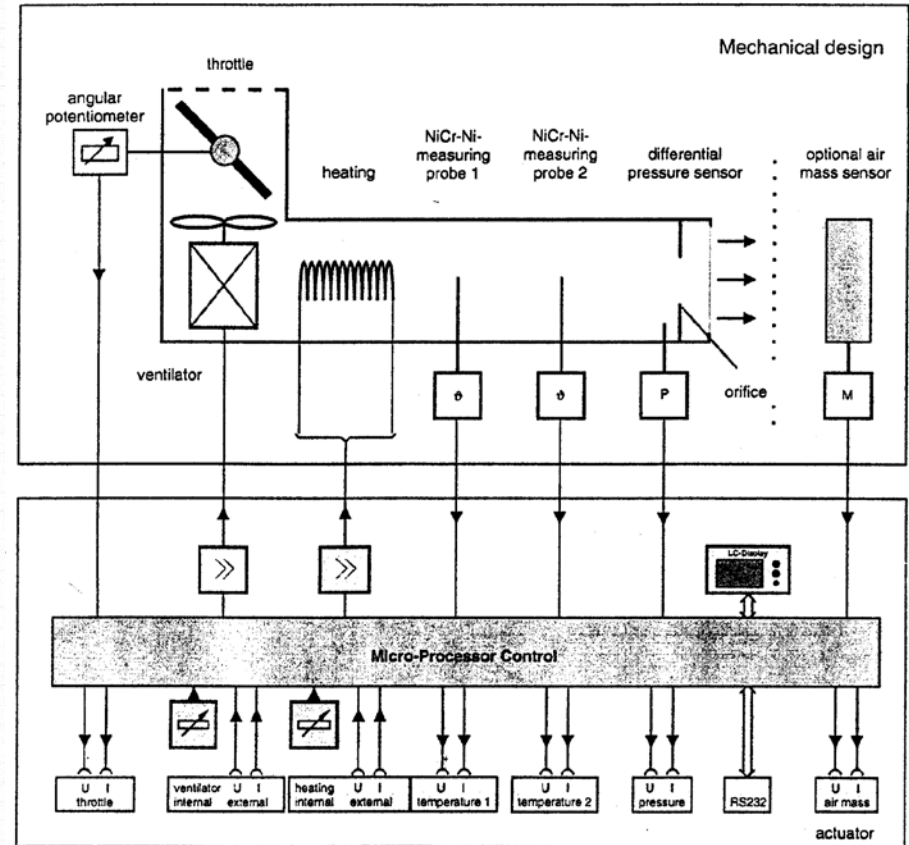
The plant identification (actuators, strictly speaking plant and measuring elements) under the form of the t.f. (4.1.1) is performed for different initial and final values of the temperature ( $T_{10}$  and  $T_{20}$ ) and in different initial operating situations

The plant static gain (or the DC gain)  $k_p$  can be determined:

- by experimental approximation (the usual way) or
- by the use of the least-squares method based on Matlab programs

In the majority of possible variations, the plant static gain varies within large limits (0.5 ... 12), which ensures many possible sets of controller parameters

Fig. 4.1.5:

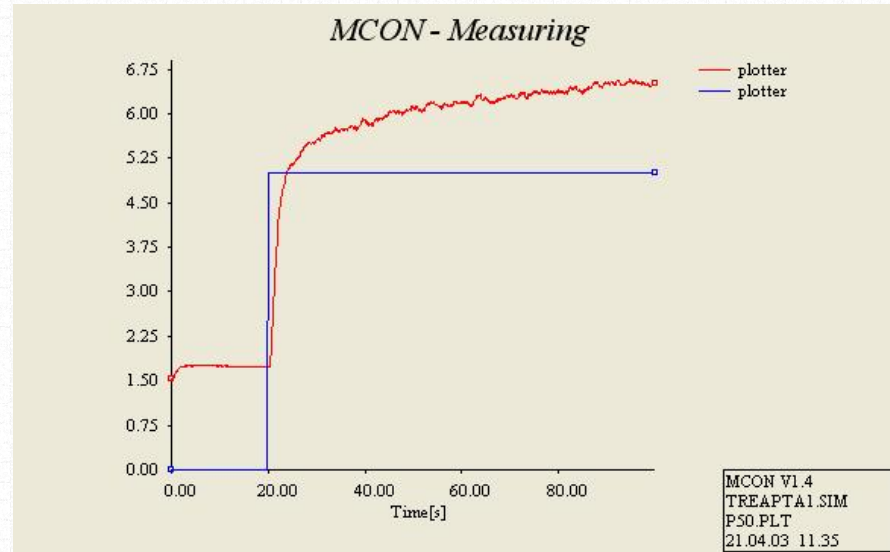


## Application (cont.)

Fig. 4.1.6 illustrates the dynamic response of the plant with respect to a step variation of the heating degree with 30% in the following initial conditions: 45% opening of air admission, heating degree 50 % and ventilator (fan) motor speed 50 %

The plant identification leads to the plant parameter values  $k_p \approx 0.93$ ,  $T \approx 2.4$  s,  $T_m \approx 0.93$  s. The controller design and tuning can be carried out on the basis of these results

Fig. 4.1.6:



## Application (cont.)

The use of a Proportional-Integral (PI) controller with the parameters tuned in terms of the Ziegler-Nichols relations with the parameters defined in the t.f. (4.1.4) with  $k_d = 0$  leads to the following values of these parameters:  $k_p = 1.92$ ,  $k_i = 0.83$

The block diagram of the control system with the PI controller implementation in MCON – Fig. 4.1.7

The variation of the control signal and the control system response (with PI controller) with respect to the step modification of the reference input followed by a step modification of the disturbance input (the fan motor speed) – Fig. 4.1.8

Fig. 4.1.7:

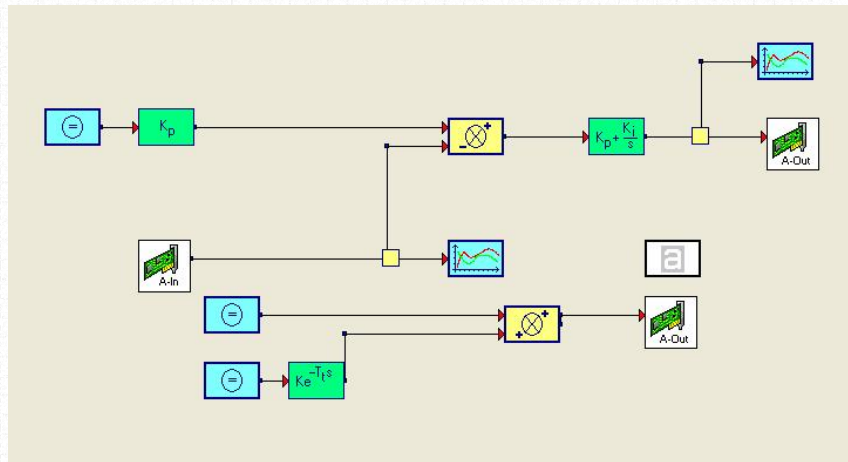
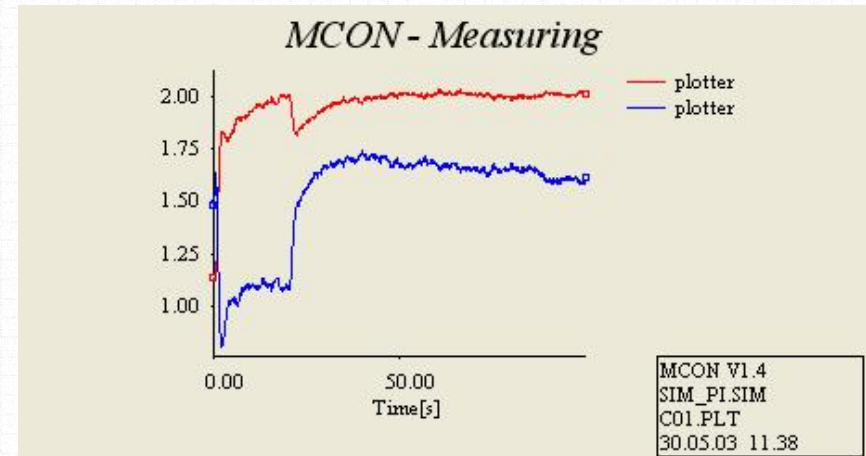


Fig. 4.1.8:





# 2

## **Modulus Optimum method and Symmetrical Optimum method**



Kessler elaborated in 1958 the basic version of the Symmetrical Optimum (SO) method, and it is characterized by the fact that the open-loop t.f.  $H_0(s)$ :

$$H_0(s) = H_C(s) H_P(s) \quad (4.2.1)$$

where:

$H_C(s)$  – the controller t.f.

$H_P(s)$  – the controlled plant (or the controlled process) t.f.

leads to a double pole in the origin

This can correspond to various situations:

- the plant is characterized by an I component and the controller brings the second one in order to ensure the condition of zero steady-state control error and zero static coefficient
- the plant does not contain any I component, but the requirement for zero control error with respect to the ramp modification of the reference input leads to the necessity that the controller should bring the two I components

The tuning methods presented in this sub-chapter are applied mainly to fast processes (plants)

## A short overview on the Symmetrical Optimum method

The basic version of the SO method accepts that the controlled plant t.f. is expressed as:

$$H_P(s) = \frac{k_p}{(1+sT_\Sigma) + \prod_{v=1}^n (1+sT_v)} \quad (4.2.2)$$

where:

$T_\Sigma$  – includes the effects of the small time constants of controlled plant

$T_v$  – large time constants of the plant ( $v = 1 \dots n$ )

For the large time constants of the controlled plant  $T_v$ , the t.f. (4.2.2) – transferred into the frequency domain – for large values of the frequency  $\omega$ , the following approximation will be accepted:

$$1 + j\omega T_v \approx j\omega T_v \quad (4.2.4)$$

The main drawback of the SO method: the relatively small phase margin of the control loop,  $\varphi_m \approx 36^\circ$  – reflected in the increased sensitivity with respect to parametric modifications

## A practical version of the Symmetrical Optimum method

Many remarkable applications are related to the field of electrical drives, characterized by t.f.s expressed as benchmark type plants:

$$H_P(s) = \frac{k_P}{s(1 + sT_\Sigma)} \quad (4.2.19)$$

The use of a PI or a PID controller having the t.f. (4.2.21) and (4.2.22), respectively:

$$H_C(s) = \frac{k_C}{s}(1 + sT_C) \quad (4.2.21)$$

or

$$H_C(s) = \frac{k_C}{s}(1 + sT_C)(1 + sT_C') \quad (4.2.22)$$

with  $T_C' = T_1$  (pole-zero cancellation), simplifies enough the design steps

## Extensions of the Symmetrical Optimum method

The “optimal performance” guaranteed by the SO method – namely  $\sigma_1 \approx 43\%$  (overshoot),  $t_s \approx 16.5T_\Sigma$  (settling time),  $t_1 \approx 3.1T_\Sigma$  (first settling time) and a small phase margin,  $\varphi_m \approx 36^\circ$  (the main drawback of the SO method) – are seldom acceptable, so the retuning of the controller parameters or the use of adequate designed reference filters are strongly recommended

Efficient ways for performance enhancement are based on two extensions of the SO method, the **Extended Form of the Symmetrical Optimum Method** (the ESO method), and the **Double Parameterization of the Symmetrical Optimum Method** (the 2p-SO method)



## The Extended Symmetrical Optimum method (the ESO method)

The ESO method is dedicated mainly to positioning systems with processes characterized by the t.f.s with an integral (I) component. Applying the optimization relations

$$\sqrt{\beta}a_0a_2 = a_1^2, \sqrt{\beta}a_1 a_3 = a_2^2 \quad (4.2.24)$$

leads to the characteristic t.f.s (open-loop and closed-loop):

$$H_0(s) = \frac{1 + \beta T_\Sigma s}{\beta \sqrt{\beta} T_\Sigma^2 s^2 (1 + T_\Sigma s)} \quad (4.2.25)$$

$$H_r(s) = H_w(s) = \frac{1 + \beta T_\Sigma s}{\beta \sqrt{\beta} T_\Sigma^3 s^3 + \beta \sqrt{\beta} T_\Sigma^2 s^2 + \beta T_\Sigma s + 1}$$

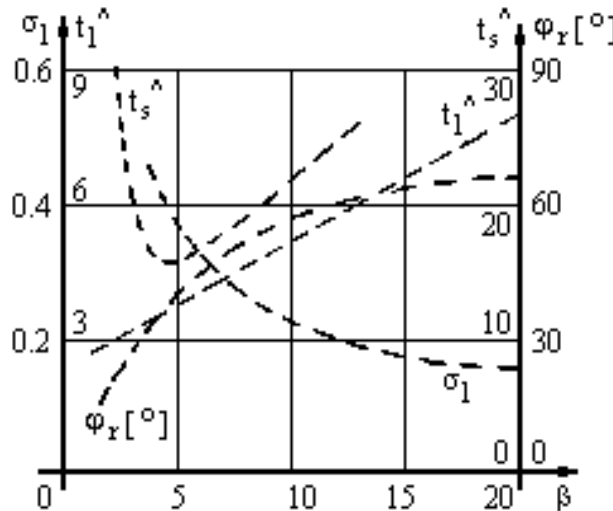
## The Extended Symmetrical Optimum method (the ESO method) (cont.)

The ESO method ensures the compact tuning relations for the parameters, general form:

$$k_c = \frac{1}{k_p \beta \sqrt{\beta T_\Sigma^2}}, T_c = \beta T_\Sigma \quad (T_c' = T_1) \quad (4.2.26)$$

This leads to significantly improved performance. Fig. 4.2.1 illustrates the main CS performance indices as function of the design parameter  $\beta$ . The ESO method also offers a good support in controller design for plants with variable parameters

Fig. 4.2.1:



The double parameterization of the SO method (the 2p-SO method)

The 2p-SO method is dedicated to driving systems (speed control) characterized by t.f.s without an I component

$$P(s) = \frac{k_P}{(1+sT_\Sigma)(1+sT_1)} \quad (a) \quad (4.2.27)$$

$$P(s) = \frac{k_P}{(1+sT_\Sigma)(1+sT_1)(1+sT_2)} \quad (b)$$

with  $T_1 > T_2 > T_\Sigma$

The 2p-SO method is based on the generalized optimization conditions (4.2.24) and on a supplementary defined parameter  $m$ :

$$m = T_\Sigma/T_1 \quad (T_\Sigma/T_1 < 1) \quad (4.2.28)$$

One of the optimized forms obtained from the characteristic t.f.s.  $H_0(s)$  and  $H_r(s)$  is:

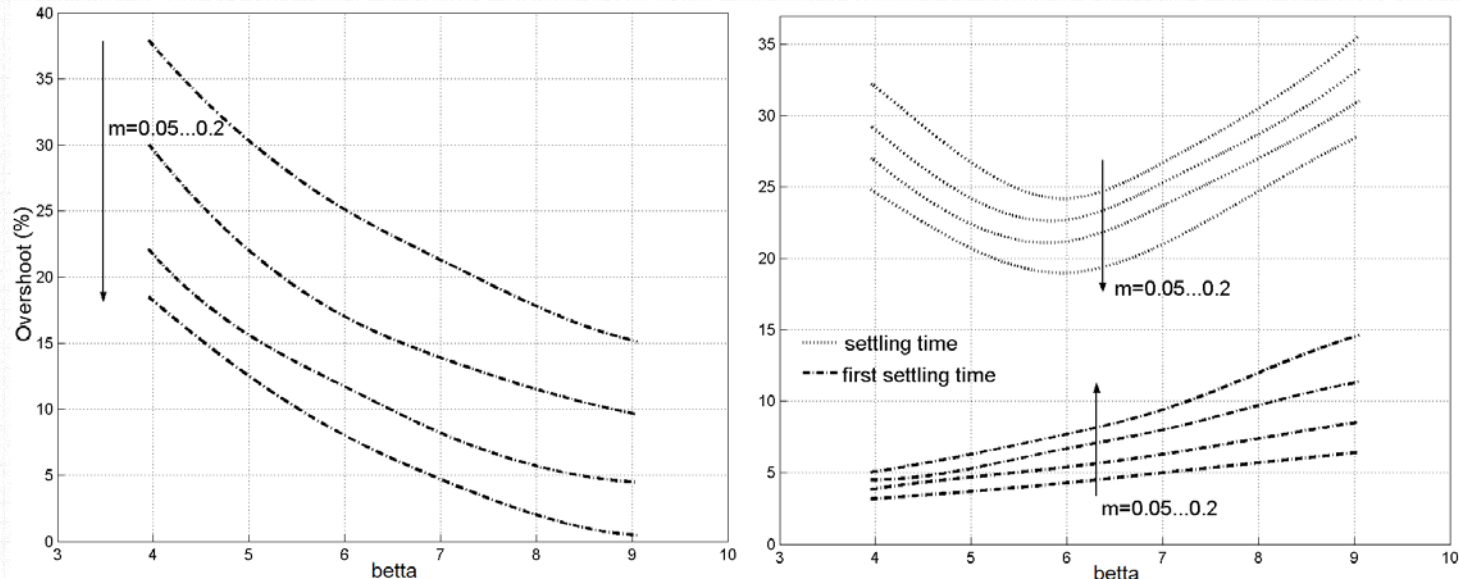
$$H_{0opt}(s) = \frac{1+\beta T_\Sigma m s}{\beta \sqrt{\beta} T_\Sigma' \frac{m}{(1+m)^2} s (1+sT_1)(1+sT_\Sigma)} \quad (4.2.29)$$



## The double parameterization of the SO method (the 2p-SO method) (cont.)

The 2p-SO method has the main advantage that can ensure the efficient disturbance rejection for a special case of servo-system application with “great and variable” moment of inertia

The CS performance indices regarding the reference input – Fig. 4.2.2:





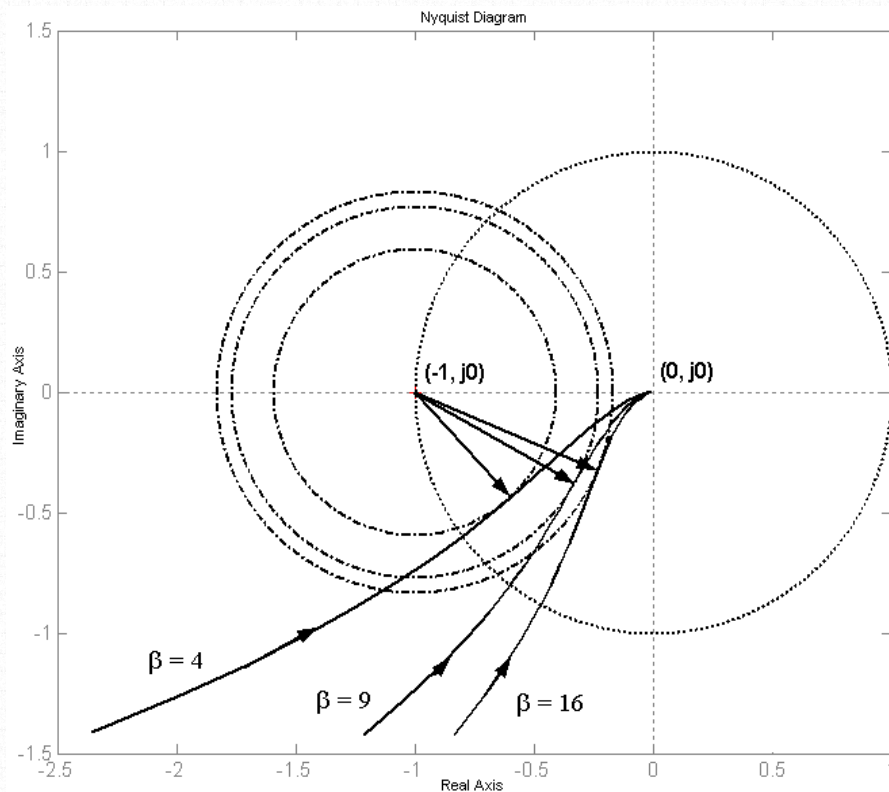
## Sensitivity analysis in the frequency domain

The CS performance indices versus  $\beta$  can be represented in a graphical form in the frequency domain

An efficient measure of the sensitivity and of the robustness of our extensions is based on the relation of the sensitivity function  $S_0(s)$  and of the complementary sensitivity function  $T_0(s)$ , the Nyquist plots and the  $M_{S_0}(s) = f(\beta)$  circles, and the values of  $M_{S_0}^{-1}$  versus  $\beta$  and/or the Bode diagrams for different values of  $\beta$  and  $m$

## Sensitivity analysis in the frequency domain (cont.)

For example, Fig. 4.2.4 illustrates the Nyquist curves, the  $M_{S0} = f(\beta)$  circles and the  $M_{S0}^{-1} = f(\beta)$  circles for the ESO method considering three representative values of  $\beta$ , namely  $\beta \in \{4, 9, 16\}$ :

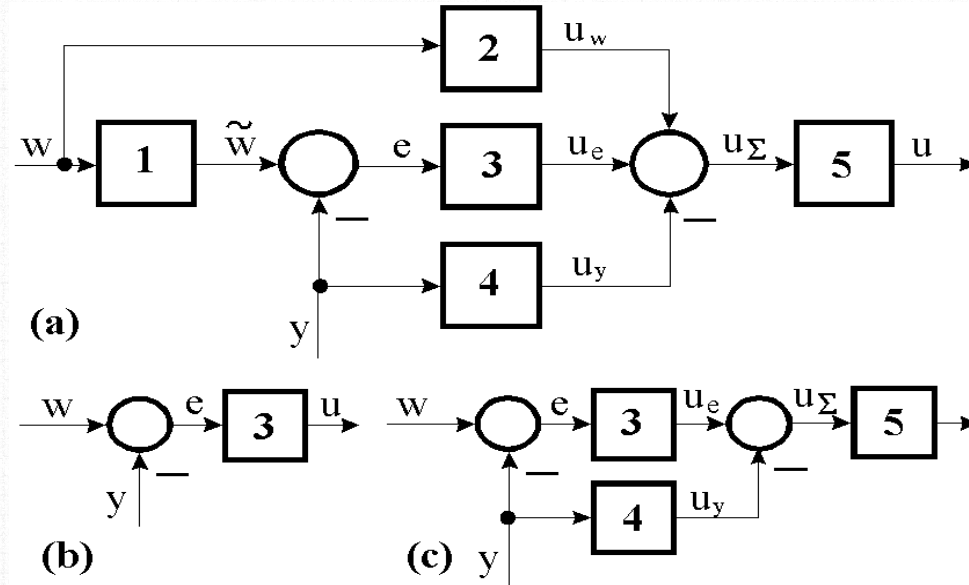


## Further performance enhancement. Alternative controller structures

Both extensions are applied incorporated in alternative control structures and algorithms

Such applications are exemplified: Fig. 4.2.6, plus particular case of control structure (CS) containing controllers with nonhomogeneous dynamics with respect to the two inputs – Fig. 4.2.7

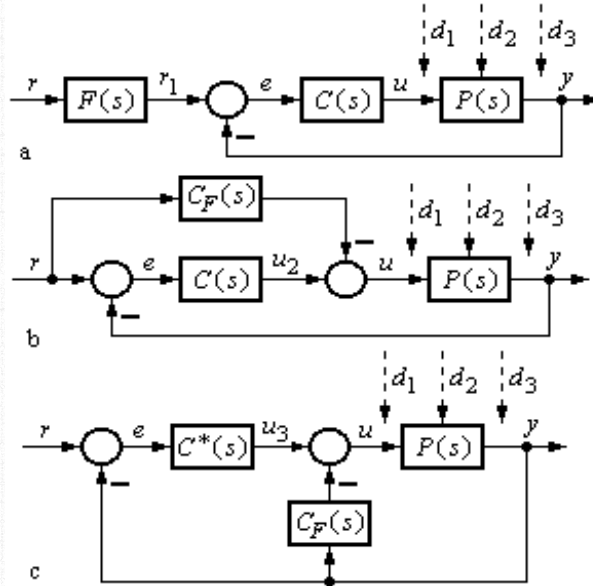
Fig. 4.2.6:





## Further performance enhancement. Alternative controller structures (cont.)

Fig. 4.2.7:



The control system behavior in the relation  $r \rightarrow r_1 \rightarrow y$  is given by the following t.f. and the closed-loop system has an oscillatory behavior only for  $\beta < 9$ :

$$\tilde{H}_r(s) = \frac{1}{(1 + \sqrt{\beta} T_\Sigma s)[1 + (\beta - \sqrt{\beta}) T_\Sigma s + \beta T_\Sigma^2 s^2]} \quad (4.2.35)$$

## Equivalency of 1-DOF (PID) and 2-DOF controllers

The PI or PID controllers (with/without reference filters) can be restructured in form of the 2-DOF controller, and vice-versa, where the presence of a conventional controller can be highlighted. Two types of such rearranged PI(D) structures are detailed in Fig. 4.2.7 (b) and (c)

The rearrangements allow take into account the design experience in the case of PI and PID controllers. For example, if the controller in Fig. 4.2.7 (b) is characterized by a continuous t.f. with the “traditional” tuning parameters  $\{k_R, T_i, T_d, T_f\}$ , the t.f.s of the equivalent blocks are:

$$C(s) = \frac{u(s)}{e(s)} = k_R \left( 1 + \frac{1}{sT_i} + \frac{sT_d}{1+sT_f} \right) \quad (4.2.36)$$

$$C_F(s) = \frac{u_f(s)}{r(s)} = k_R \left( \alpha_1 + \alpha_2 \frac{sT_d}{1+sT_f} \right)$$

## Equivalency between 1-DOF (PID) and 2-DOF controllers (cont.)

The connections of these blocks are illustrated in Table 4.2.1, which depends on the values of  $\alpha_1$  and  $\alpha_2$  (parameters)

The choice of a certain representation of the controller depends on:

- the structure of the available controller
- the adopted algorithmic design method and the result of this design

Table 4.2.1:

Fig. 4.2.7(a)	F(s)	-	F(s)C(s)	C(s)	Remarks	
Fig. 4.2.7(b)	-	C <sub>F</sub>	C(s)−C <sub>F</sub> (s)	C(s)	-	
Fig. 4.2.7(c)	-	C <sub>P</sub>	C*(s)	C*(s)+C <sub>P</sub> (s)	-	
α <sub>1</sub>	α <sub>2</sub>	-	-	(ref. channel)	(feedback)	
0	0	1	0	PID	PID	1-DOF controller
0	1	PDL2	DL1	PI	PID	1-DOF with non-homogenous behavior
1	0	PD2L2	P	PID-L1	PID	
1	1	PL2	PDL2	I	PID	
α <sub>1</sub>	α <sub>2</sub>	PID controller with pre-filtering (2-DOF controller)				



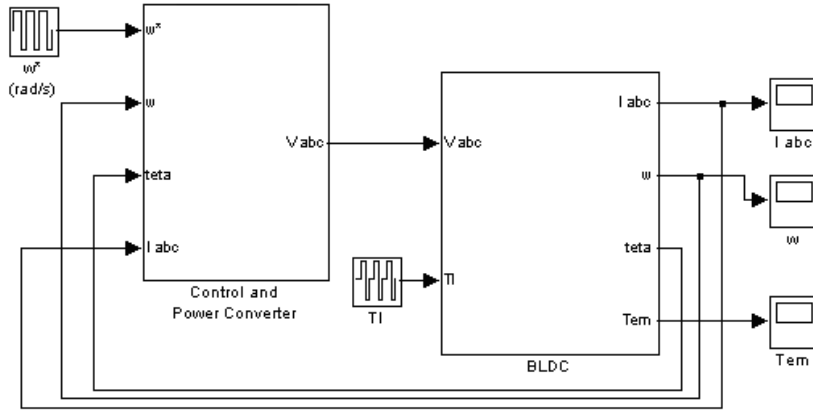
## Application 4.2.1

Let us consider the representative controlled plants (processes) in the field of electrical drives exemplified by the Direct Current (DC) motors (DC-ms) and by Brushless Direct Current (BLDC) motors (BLDC-ms) with an internal control loop

The ESO method will be applied as follows to design the controller in the outer control loop (the speed control loop) in a cascade control system structure.

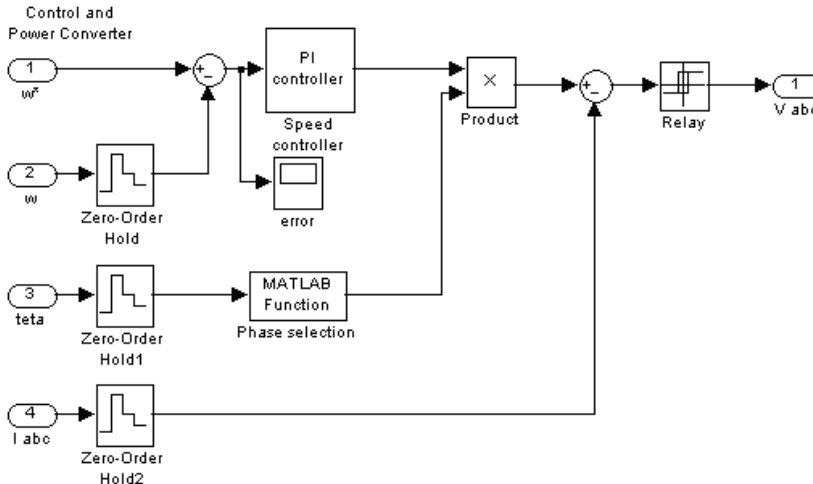
In the symmetrical operating mode, the mathematical models of BLDC-m and DC-m are very close. This aspect leads to similarities in the controller design and to cost-effective implementations. In case of BLDC-m based drives the current switching is obtained by specialized converters with commutation time determined by the position of the rotor. The block diagram of BLDC-m with permanent magnets contains the PWM inverter, the current and speed sensors and the controllers. An on-off controller with hysteresis is used in the inner current control loop; the phase selection block ensures the proper switching of the phases and the initialization. A PI(D) controller is used in the main speed control loop. The cascade CS structure – Fig. 4.2.8:

## Application 4.2.1 (cont.)



This application simulates a winding process with VMI and constant linear speed,  $v_t(t) = \text{const}$  (Fig. 4.2.9), where the reference input is the linear speed of the enrolled material which must be constant

The desired angular speed ( $\omega$ ) must be correlated with the modification of the working roll radius  $r_r$



The controller parameters must be tuned and retuned as well

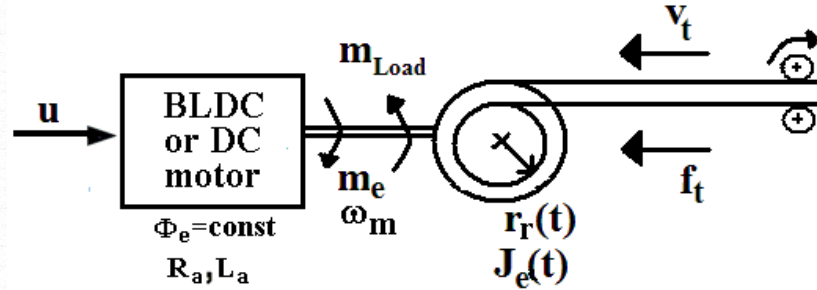
To treat this first aspect, the following condition must be fulfilled:

$$v_t(t) = \text{const} \Rightarrow r(t) = k/r_r(t) \quad (4.2.38)$$

### Application 4.2.1 (cont.)

The measurement of  $r_t(t)$  enables the continuous modification of the moment of inertia expressed as:

$$J_e(t) = \frac{1}{2} \rho \pi l r_r^4 \quad (4.2.39)$$



The inner loop can be characterized generally by simplified benchmark type second-order t.f.s connected to the operating point. The speed controller is of PI type, with an I component to ensure good tracking properties. The resulting open-loop t.f. with a double pole in the origin (imposed in the SO method):

$$H_0(s) = C(s)P(s) = \frac{k_0(1+sT_C)}{s^2(1+sT_\Sigma)} \quad (4.2.40)$$



## Application 4.2.1 (cont.)

with:

$$C(s)=H_c(s) \text{ and } P(s)=H_p(s)$$

$T_c = T_1 = T_m$  – the mechanical time constant, which is time-variable and must be compensated for

$$k_0=k_pk_c, \quad T_1 \gg T_\Sigma$$

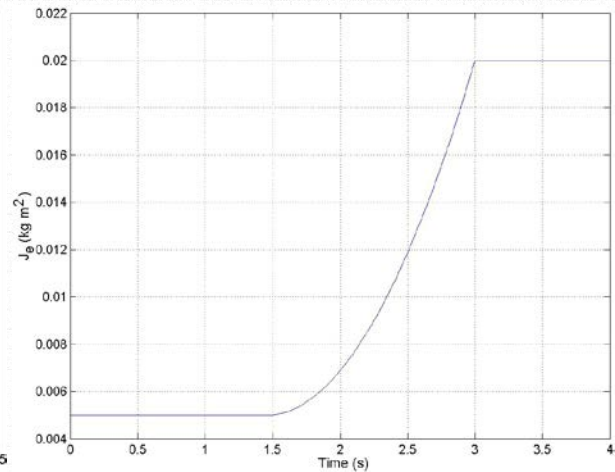
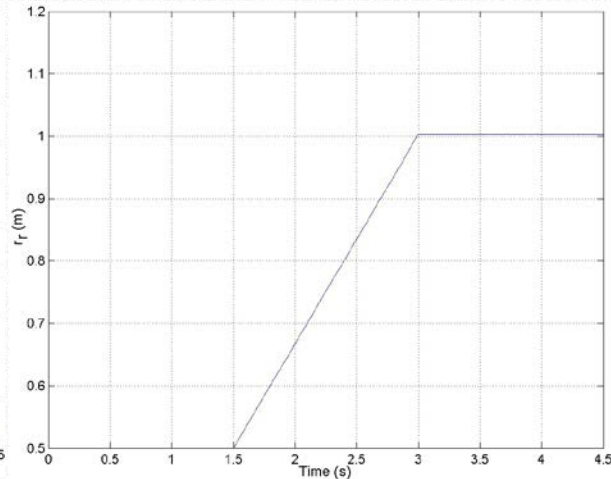
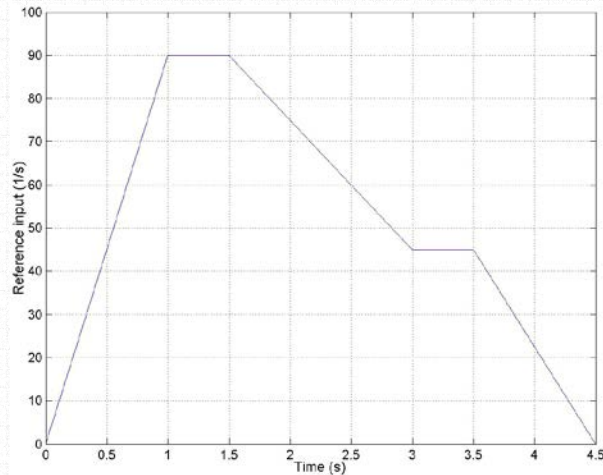
A BLDC-m-based servo system with VMI characterized by the following parameters is considered:

- $p=2$
- $R_a = 1\Omega$
- $L_a = 0.02\text{ H}$
- $V_{DC} = 220\text{ V}$
- $J_{e0} = 0.005\text{ kg m}^2$

The inner control loop ensures a second-order (with lag) process behavior characterized by (4.2.27) (a) with  $k_P = 40, T_1 = 0.015\text{ s}$

## Application 4.2.1 (cont.)

The tuning conditions (4.2.26) specific to the ESO method are applied setting the value  $\beta = 12$  for the average value for  $J_e(t)$ , without parameter adaption and ARW measure. The simulation scenario consists of a starting regime (starting the BLDC motor, from 0 to 1 s), the constant reference for the linear speed (from 1 s to 1.5 s), the winding process starting (from 1.5 s to 3 s); the winding process stopping (from 3 s to 3.5 s) and the stopping regime for the BLDC-m, (from 3.5 s to 4.5 s). These regimes aim the modification of the angular speed  $\omega$  to ensure the desired linear speed  $v_t$  accompanied by increasing of the linear speed reference input  $r(t)$ . Figs. 4.2.10, 4.2.11 & 4.2.12 synthesize a part of the simulation results:





Thank you very much for your attention!

Prof. Dr. Ing. Dipl. Math. Dr. h.c. mult. Radu-Emil Precup  
<https://www.aut.upt.ro/~rprecup/>